ELSEVIER

International Journal of Solids and Structures 41 (2004) 5285–5300

INTERNATIONAL JOURNAL OF SOLIDS and STRUCTURES

www.elsevier.com/locate/ijsolstr

Green's functions for anti-plane problems in piezoelectric media with a finite crack

B.J. Chen [a,*], K.M. Liew [a,b], Z.M. Xiao [b]

[a] *Nanyang Centre for Supercomputing and Visualisation, Nanyang Technological University, Nanyang Avenue, Singapore 639798, Singapore*

[b] *School of Mechanical and Production Engineering, Nanyang Technological University, Nanyang Avenue, Singapore 639798, Singapore*

Received 2 July 2003; received in revised form 3 April 2004
Available online 12 May 2004

Abstract

Based on the complex variable method and the perturbation technique, Green's functions for the anti-plane problems in an infinite piezoelectric medium with a crack under remote uniform loadings are derived. The analysis is conducted on the electrically unified crack boundary condition with the introduction of the electric crack condition parameter that can describe all the electric crack boundary conditions. The two ideal crack boundary conditions, namely, the electrically impermeable and permeable crack assumptions are obtained as two special cases for the current solution. The explicit expressions of the mechanical and electrical fields produced by a line-force, a line-charge and a screw dislocation are derived and the field intensity factors are calculated. The image forces on the dislocation due to the crack and the remote uniform loadings are computed as functions of dislocation position and material constant combinations. Numerical examples are performed to show how the electric crack condition parameter affects the field intensity factors and the force on the dislocation.

Keywords: Green's function; Piezoelectric; Crack; Unified boundary condition

1. Introduction

Piezoelectric materials have been widely used to diverse areas, such as electromechanical transducers, electronic packaging, thermal sensors and medical ultrasonic imaging. However, various types of defects existed in piezoelectric materials, such as dislocations and cracks, can adversely influence the performance of these piezoelectric devices. The reliability problem emerges and requires a better understanding of the fracture behavior of these materials. A lot of theoretical results have been presented in the literatures. Deeg (1980) analyzed the dislocation, crack, and inclusion problems in piezoelectric solids. He assumed that the electric is impermeable across the crack and ignores the electric field within the crack. This is the so-called

* Corresponding author. Tel.: +65-67904072; fax: +65-67936763.
E-mail address: mbjchen@ntu.edu.sg (B.J. Chen).

0020-7683/$ - see front matter © 2004 Elsevier Ltd. All rights reserved.
doi:10.1016/j.ijsolstr.2004.04.010

electrically impermeable crack assumption, which was widely used to investigate the crack problem in piezoelectric media to simplify analysis, see, for example, the work of Pak (1990a, 1992), Sosa (1991), Wang (1992), Park and Sun (1995), Qin and Yu (1997), Zhong and Meguid (1997a,b), Qin (2000), Kwon and Lee (2002). In fact, cracks in the engineering are usually filled with air or vacuum, which means that both the normal component of electric displacement and the tangential component of the electric field are continuous across the crack faces (Parton, 1976). This is the so-called electrically permeable crack assumption. As pointed out by McMeeking (1989) and Dunn (1994), the impermeable crack assumption is physically untenable, and thus will lead to erroneous results, for example, an artificial singularity of electric field solely in the presence of electric loading. In order to consider the electric inside the crack, Sosa and Khutoryansky (1996), Zhang and Tong (1996), Zhang et al. (1998, 2002) investigated the crack problem by first solving the elliptical cavity problem and then reducing the cavity to a crack.

In the paper, we adopt the unified crack boundary condition (Kwon, 2003; Wang and Mai, 2003) that can describe more reasonable cracks. The obtained results can be degenerated into both the electrically impermeable and electrically permeable assumptions as special cases. Based on the continuous conditions, the anti-plane problems of an infinite piezoelectric medium that contains a finite crack subjected to a line-force, a line-charge and a dislocation near the crack are addressed by means of the complex variable method and the perturbation technique.

2. Statement of the problem

Let us consider the physical problem as shown in Fig. 1. A screw dislocation is located at a point z_d around a finite crack of length $2a$ in an infinite piezoelectric medium. The medium is under remote uniform anti-plane stresses and in-plane electric displacement fields. The dislocation is assumed to be straight and infinitely long in the z-direction, suffering a finite discontinuity in the displacement and electric potential across the slip plane. The dislocation has a line-force and a line-charge along its core. The piezoelectric medium considered here is transversely isotropic with hexagonal symmetry, which has an isotropic basal plane of xy-plane and a poling direction of z-axis.

In a linear piezoelectric medium, the governing field equations and constitutive relations at constant temperature can be written as

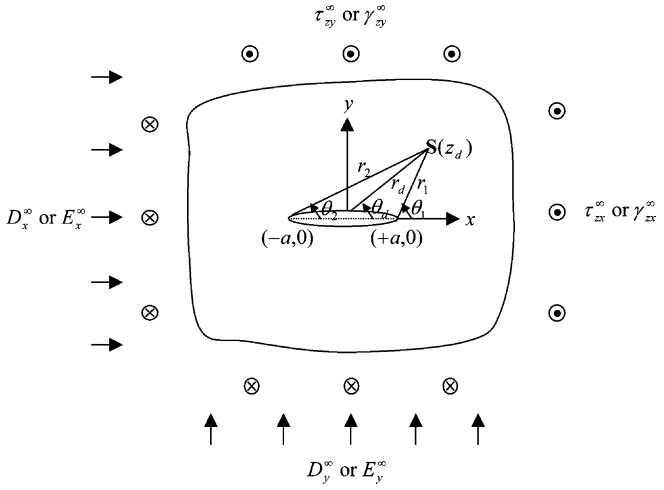

Fig. 1. A screw dislocation around a finite crack in an infinite piezoelectric medium under remote loadings.

$$\sigma_{ij,j} = 0, \qquad D_{i,i} = 0, \tag{2.1}$$

$$\sigma_{ij} = c_{ijkl}u_{k,l} - e_{kij}E_k, \qquad D_i = e_{ikl}u_{k,l} + \varepsilon_{ik}E_k, \tag{2.2}$$

where σ_{ij}, u_i, D_i and E_i are stress, displacement, electric displacement and electric fields, respectively. c_{ijkl}, e_{kij} and ε_{ij} are the corresponding elastic, piezoelectric and dielectric constants which satisfy the following relations:

$$c_{ijkl} = c_{klij} = c_{ijlk} = c_{jikl}, \qquad e_{kij} = e_{kji}, \qquad \varepsilon_{ik} = \varepsilon_{ki}. \tag{2.3}$$

For the current problem, the displacement w is coupled only with the in-plane electric field E_x and E_y, those variables are independent of the longitudinal coordinate z, such that

$$w = w(x,y), \qquad E_x = E_x(x,y), \qquad E_y = E_y(x,y). \tag{2.4}$$

The governing field equations and constitutive relations in (2.1) and (2.2) are thus reduced to

$$\frac{\partial \sigma_{zx}}{\partial x} + \frac{\partial \sigma_{zy}}{\partial y} = 0, \qquad \frac{\partial D_x}{\partial x} + \frac{\partial D_y}{\partial y} = 0, \tag{2.5}$$

$$\begin{aligned} \sigma_{zx} &= c_{44}\frac{\partial w}{\partial x} + e_{15}\frac{\partial \varphi}{\partial x}, \qquad \sigma_{zy} = c_{44}\frac{\partial w}{\partial y} + e_{15}\frac{\partial \varphi}{\partial y}, \\ D_x &= e_{15}\frac{\partial w}{\partial x} - \varepsilon_{11}\frac{\partial \varphi}{\partial x}, \qquad D_y = e_{15}\frac{\partial w}{\partial y} - \varepsilon_{11}\frac{\partial \varphi}{\partial y}, \end{aligned} \tag{2.6}$$

where $\varphi = \varphi(x,y)$ is the electric potential and

$$E_x = -\frac{\partial \varphi}{\partial x}, \qquad E_y = -\frac{\partial \varphi}{\partial y}. \tag{2.7}$$

Substituting (2.6) into (2.5), we have

$$c_{44}\nabla^2 w + e_{15}\nabla^2 \varphi = 0, \qquad e_{15}\nabla^2 w - \varepsilon_{11}\nabla^2 \varphi = 0, \tag{2.8}$$

where ∇^2 is the two-dimensional Laplacian operator. The above equations can be satisfied if we choose

$$\nabla^2 w = 0, \qquad \nabla^2 \varphi = 0. \tag{2.9}$$

If we let the harmonic functions w and φ be the imaginary parts of some complex potentials of the complex variable $z = x + \mathrm{i}y = r\,\mathrm{e}^{\mathrm{i}\theta}$, or

$$w = \mathrm{Im}[u(z)], \qquad \varphi = \mathrm{Im}[\phi(z)], \tag{2.10}$$

where "Im" stands for the imaginary part, then the strain and electric fields can be expressed as

$$\gamma_{zy} + \mathrm{i}\gamma_{zx} = W(z), \tag{2.11}$$

$$E_y + \mathrm{i}E_x = -\Phi(z), \tag{2.12}$$

while the stress and electric displacement fields can be expressed as

$$\tau_{zy} + \mathrm{i}\tau_{zx} = c_{44}W(z) + e_{15}\Phi(z), \tag{2.13}$$

$$D_y + \mathrm{i}D_x = e_{15}W(z) - \varepsilon_{11}\Phi(z), \tag{2.14}$$

where $W(z) = u'(z)$, $\Phi(z) = \phi'(z)$, the prime denotes the derivative with respect to the argument z.

The far field boundary conditions are

$$\tau_{zx}(x, \pm\infty) = \tau_{zx}^{\infty}, \qquad \tau_{zy}(x, \pm\infty) = \tau_{zy}^{\infty}, \tag{2.15}$$

$$D_x(x,\pm\infty) = D_x^{\infty}, \qquad D_y(x,\pm\infty) = D_y^{\infty}, \tag{2.16}$$

where τ_{zx}^{∞}, τ_{zy}^{∞}, D_x^{∞} and D_y^{∞} are uniform shear stress and electric displacement field respectively, as shown in Fig. 1.

The mechanical boundary conditions at the crack surface are

$$\tau_{zy}(x)^{+} = \tau_{zy}(x)^{-} = 0, \quad |x| < a, \tag{2.17}$$

$$w(x)^{+} = w(x)^{-}, \quad |x| \geqslant a, \tag{2.18}$$

where the superscript "+" and "−" refer, respectively, to the upper and lower crack surfaces.

The electric boundary conditions at the crack surface are

$$E_y(x)^{+} = E_y(x)^{-} = C_r E_0(x), \quad |x| < a, \tag{2.19}$$

$$\varphi(x)^{+} = \varphi(x)^{-}, \quad |x| \geqslant a, \tag{2.20}$$

where $E_0(x)$ is the boundary value of $E_y(z)$ on the crack faces due to the dislocation and the far field loading without the disturbance of the crack. C_r is referred to the electric crack condition parameter. Eqs. (2.19) and (2.20) are referred to electrically unified crack boundary condition hereafter (Wang and Mai, 2003; Kwon, 2003). The solutions based on this condition will correctly recover both the impermeable and permeable crack solutions as limiting cases.

3. Solution of the problem

We assume that a screw dislocation with Burgers vector b_z, a line-force p, a line-charge q, and an electric potential jump b_φ, are located at a point z_d near the crack under remotely uniform loadings (Fig. 1), Based on the perturbation technique, the corresponding complex potentials $W(z)$ and $\Phi(z)$ can be written as

$$W(z) = W_0(z) + W_1(z), \tag{3.1}$$

$$\Phi(z) = \Phi_0(z) + \Phi_1(z), \tag{3.2}$$

where $W_1(z)$ and $\Phi_1(z)$ are the analytical functions corresponding the perturbed field due to the existing of the crack; $W_0(z)$ and $\Phi_0(z)$ are associated with the unperturbed fields without the crack, they can be written as

$$W_0(z) = (A_1 + \mathrm{i}A_2) + (A_3 + \mathrm{i}A_4)/(z - z_d), \tag{3.3}$$

$$\Phi_0(z) = (B_1 + \mathrm{i}B_2) + (B_3 + \mathrm{i}B_4)/(z - z_d). \tag{3.4}$$

The A_1, A_2, A_3, A_4, B_1, B_2, B_3 and B_4 in the above equations are constants to be determined by the characteristics of dislocation and the far field conditions. The remotely uniform loadings requires that

$$\tau_{zy} + \mathrm{i}\tau_{zx} = c_{44} W_0(z \to \infty) + e_{15}\Phi_0(z \to \infty), \tag{3.5}$$

$$D_y + \mathrm{i}D_x = e_{15} W_0(z \to \infty) - \varepsilon_{11}\Phi_0(z \to \infty). \tag{3.6}$$

The force and charge balances require that

$$\oint_C \tau_{zj} n_j \,\mathrm{d}l = -p, \oint_C D_j n_j \,\mathrm{d}l = q. \tag{3.7}$$

For any Burgers circuit enclosing only the dislocation, we obtain

$$\oint_C \frac{\partial w}{\partial l}\,\mathrm{d}l = b_z, \quad \oint_C \frac{\partial \varphi}{\partial l}\,\mathrm{d}l = b_\varphi. \tag{3.8}$$

The substitution of (2.10) into (3.5) and (3.6) results in

$$A_1 = \frac{\tau_{zy}^\infty + e_{15}E_y^\infty}{c_{44}}, \qquad A_2 = \frac{\tau_{zx}^\infty + e_{15}E_x^\infty}{c_{44}}, \tag{3.9a}$$

$$B_1 = -E_y^\infty, \qquad B_2 = -E_x^\infty, \tag{3.10a}$$

for Case a: $\tau(x,\pm\infty) = \tau_{zy}^\infty + \mathrm{i}\tau_{zx}^\infty$ and $E(x,\pm\infty) = E_y^\infty + \mathrm{i}E_x^\infty$, and

$$A_1 = \frac{\varepsilon_{11}\tau_{zy}^\infty + e_{15}D_y^\infty}{c_{44}\varepsilon_{11} + e_{15}^2}, \qquad A_2 = \frac{\varepsilon_{11}\tau_{zx}^\infty + e_{15}D_x^\infty}{c_{44}\varepsilon_{11} + e_{15}^2}, \tag{3.9b}$$

$$B_1 = \frac{e_{15}\tau_{zy}^\infty - c_{44}D_y^\infty}{c_{44}\varepsilon_{11} + e_{15}^2}, \qquad B_2 = \frac{e_{15}\tau_{zx}^\infty - c_{44}D_x^\infty}{c_{44}\varepsilon_{11} + e_{15}^2}, \tag{3.10b}$$

for Case b: $\tau(x,\pm\infty) = \tau_{zy}^\infty + \mathrm{i}\tau_{zx}^\infty$ and $D(x,\pm\infty) = D_y^\infty + \mathrm{i}D_x^\infty$, and

$$A_1 = \gamma_{zy}^\infty, \qquad A_2 = \gamma_{zx}^\infty, \tag{3.9c}$$

$$B_1 = -E_y^\infty, \qquad B_2 = -E_x^\infty, \tag{3.10c}$$

for Case c: $\gamma(x,\pm\infty) = \gamma_{zy}^\infty + \mathrm{i}\gamma_{zx}^\infty$ and $E(x,\pm\infty) = E_y^\infty + \mathrm{i}E_x^\infty$, and

$$A_1 = \gamma_{zy}^\infty, \qquad A_2 = \gamma_{zx}^\infty, \tag{3.9d}$$

$$B_1 = \frac{e_{15}\gamma_{zy}^\infty - D_y^\infty}{\varepsilon_{11}}, \qquad B_2 = \frac{e_{15}\gamma_{zx}^\infty - D_x^\infty}{\varepsilon_{11}}, \tag{3.10d}$$

for Case d: $\gamma(x,\pm\infty) = \gamma_{zy}^\infty + \mathrm{i}\gamma_{zx}^\infty$ and $D(x,\pm\infty) = D_y^\infty + \mathrm{i}D_x^\infty$. The substitution of (2.10) into (3.7) and (3.8) results in

$$A_3 = \frac{b_z}{2\pi}, \qquad A_4 = \frac{1}{2\pi}\frac{e_{15}q - \varepsilon_{11}p}{c_{44}\varepsilon_{11} + e_{15}^2}, \tag{3.11}$$

$$B_3 = \frac{b_\varphi}{2\pi}, \qquad B_4 = -\frac{1}{2\pi}\frac{c_{44}q + e_{15}p}{c_{44}\varepsilon_{11} + e_{15}^2}. \tag{3.12}$$

With reference to (2.13), the condition (2.17) yields

$$c_{44}[W(x)^+ + \overline{W}(x)^-] + e_{15}[\Phi(x)^+ + \overline{\Phi}(x)^-] = 0, \quad |x| < a \tag{3.13}$$

and

$$c_{44}[W(x)^- + \overline{W}(x)^+] + e_{15}[\Phi(x)^- + \overline{\Phi}(x)^+] = 0, \quad |x| < a \tag{3.14}$$

where the over-bar denotes conjugate. The subtraction and addition of Eqs. (3.13) and (3.14), respectively, give

$$c_{44}\{[W(x) - \overline{W}(x)]^+ - [W(x) - \overline{W}(x)]^-\} + e_{15}\{[\Phi(x) - \overline{\Phi}(x)]^+ - [\Phi(x) - \overline{\Phi}(x)]^-\} = 0, \quad |x| < a \tag{3.15}$$

and

$$c_{44}\{[W(x)+\overline{W}(x)]^{+}+[W(x)+\overline{W}(x)]^{-}\}+e_{15}\{[\Phi(x)+\overline{\Phi}(x)]^{+}+[\Phi(x)+\overline{\Phi}(x)]^{-}\}=0,\quad |x|<a \tag{3.16}$$

Substituting (3.1) and (3.2) into (3.15) and (3.16), we obtain

$$c_{44}\{[W_1(x)-\overline{W}_1(x)]^{+}-[W_1(x)-\overline{W}_1(x)]^{-}\}+e_{15}\{[\Phi_1(x)-\overline{\Phi}_1(x)]^{+}-[\Phi_1(x)-\overline{\Phi}_1(x)]^{-}\}=0,\quad |x|<a \tag{3.17}$$

and

$$c_{44}\{[W_1(x)+\overline{W}_1(x)]^{+}+[W_1(x)+\overline{W}_1(x)]^{-}\}+e_{15}\{[\Phi_1(x)+\overline{\Phi}_1(x)]^{+}+[\Phi_1(x)+\overline{\Phi}_1(x)]^{-}\}=-2F_0(x), \tag{3.18}$$

where

$$\begin{aligned}F_0(x)&=c_{44}[2A_1+(A_3+\mathrm{i}A_4)/(x-z_d)+(A_3-\mathrm{i}A_4)/(x-\bar{z}_d)]\\&\quad+e_{15}[2B_1+(B_3+\mathrm{i}B_4)/(x-z_d)+(B_3-\mathrm{i}B_4)/(x-\bar{z}_d)].\end{aligned} \tag{3.19}$$

The solution for (3.17) and (3.18) can be written as (Muskhelishvili, 1975):

$$c_{44}W_1(z)+e_{15}\Phi_1(z)=-c_{44}F_w(z)-e_{15}F_\varphi(z), \tag{3.20}$$

where

$$\begin{aligned}F_w(z)&=A_1+\frac{A_3+\mathrm{i}A_4}{2(z-z_d)}+\frac{A_3-\mathrm{i}A_4}{2(z-\bar{z}_d)}-\frac{1}{\sqrt{z^2-a^2}}\left[A_1z+\frac{A_3+\mathrm{i}A_4}{2}\left(\frac{\sqrt{z_d^2-a^2}}{z-z_d}+1\right)\right.\\&\quad\left.+\frac{A_3-\mathrm{i}A_4}{2}\left(\frac{\sqrt{\bar{z}_d^2-a^2}}{z-\bar{z}_d}+1\right)\right],\end{aligned} \tag{3.21}$$

$$\begin{aligned}F_\varphi(z)&=B_1+\frac{B_3+\mathrm{i}B_4}{2(z-z_d)}+\frac{B_3-\mathrm{i}B_4}{2(z-\bar{z}_d)}-\frac{1}{\sqrt{z^2-a^2}}\left[B_1z+\frac{B_3+\mathrm{i}B_4}{2}\left(\frac{\sqrt{z_d^2-a^2}}{z-z_d}+1\right)\right.\\&\quad\left.+\frac{B_3-\mathrm{i}B_4}{2}\left(\frac{\sqrt{\bar{z}_d^2-a^2}}{z-\bar{z}_d}+1\right)\right].\end{aligned} \tag{3.22}$$

In a similar way, the condition (2.19) yields

$$\Phi_1(z)=(C_r-1)F_\varphi(z). \tag{3.23}$$

The substitution of (3.23) into (3.20) arrives at

$$W_1(z)=-F_w(z)-C_r\frac{e_{15}}{c_{44}}F_\varphi(z). \tag{3.24}$$

It is noted that the above solutions automatically satisfy the conditions (2.18) and (2.20).

The solutions expressed in (3.23) and (3.24) correctly recover both the impermeable and permeable crack solutions as limiting cases. For electrically impermeable crack assumption, the crack is electrically insulating, such that $D_0=0$. This is obtained by letting $C_r=0$. The solution is then derived as

$$\begin{Bmatrix} W_1(z) \\ \Phi_1(z) \end{Bmatrix} = -\begin{Bmatrix} F_w(z) \\ F_\varphi(z) \end{Bmatrix}. \tag{3.25}$$

For electrically permeable crack assumption, the crack is electrically conducting. There is no electric potential discontinuity across the crack. This condition is fulfilled by letting $C_r = 1$. The solution is then written as

$$\begin{Bmatrix} W_1(z) \\ \Phi_1(z) \end{Bmatrix} = -\begin{Bmatrix} F_w(z) + \dfrac{e_{15}}{c_{44}} F_\varphi(z) \\ 0 \end{Bmatrix}. \tag{3.26}$$

Any possible electric crack condition is therefore unified into the parameter C_r. The solutions expressed in (3.25) and (3.26) represent, respectively, the solutions for the ideal electrically insulating crack and the ideal electrically conducting crack. They are two special cases for the electrical boundary conditions on the crack faces.

It should be noted that in the case of an elliptical flaw with a and b its major and minor axes, respectively, C_r can be associated with two parameters of the flaw, $\alpha = b/a$ and ε_0, the dielectric permittivity of the flaw medium as (Zhang and Tong, 1996)

$$C_r = \frac{1+\alpha}{1+\alpha/\beta}, \qquad \beta = \frac{\varepsilon_0}{\varepsilon_e}, \qquad \varepsilon_e = \varepsilon_{11} + \frac{e_{15}^2}{c_{44}}. \tag{3.27}$$

4. Mechanical and electrical fields

The strain and electric fields can be calculated by using (2.11) and (2.12) together with (3.1) and (3.2), which can be written as

$$\gamma_{zy} + \mathrm{i}\gamma_{zx} = (\gamma_{zy}^0 + \mathrm{i}\gamma_{zx}^0) + (\gamma_{zy}^1 + \mathrm{i}\gamma_{zx}^1), \tag{4.1}$$

$$E_y + \mathrm{i}E_x = (E_y^0 + \mathrm{i}E_x^0) + (E_y^1 + \mathrm{i}E_x^1), \tag{4.2}$$

and the stress and electric displacement fields are calculated by

$$\tau_{zy} + \mathrm{i}\tau_{zx} = (\tau_{zy}^0 + \mathrm{i}\tau_{zx}^0) + (\tau_{zy}^1 + \mathrm{i}\tau_{zx}^1), \tag{4.3}$$

$$D_y + \mathrm{i}D_x = (D_y^0 + \mathrm{i}D_x^0) + (D_y^1 + \mathrm{i}D_x^1), \tag{4.4}$$

where the variables with the superscript "0" are the unperturbed fields which are associated with $W_0(z)$ and $\Phi_0(z)$ as expressed, respectively, in Eqs. (3.3) and (3.4), and those with the superscript "1" are the perturbed fields which are associated with $W_1(z)$ and $\Phi_1(z)$ as expressed, respectively, in Eqs. (3.23) and (3.24). The unperturbed fields are given by

$$\gamma_{zy}^0 + \mathrm{i}\gamma_{zx}^0 = (A_1 + \mathrm{i}A_2) + (A_3 + \mathrm{i}A_4)/(z - z_d), \tag{4.5}$$

$$E_y^0 + \mathrm{i}E_x^0 = -(B_1 + \mathrm{i}B_2) - (B_3 + \mathrm{i}B_4)/(z - z_d), \tag{4.6}$$

$$\tau_{zy}^0 + \mathrm{i}\tau_{zx}^0 = c_{44}(\gamma_{zy}^0 + \mathrm{i}\gamma_{zx}^0) - e_{15}(E_y^0 + \mathrm{i}E_x^0), \tag{4.7}$$

$$D_y^0 + \mathrm{i}D_x^0 = \mathrm{e}_{15}(\gamma_{zy}^0 + \mathrm{i}\gamma_{zx}^0) + \varepsilon_{11}(E_y^0 + \mathrm{i}E_x^0). \tag{4.8}$$

The perturbed fields are given by

$$\gamma_{zy}^1+\mathrm{i}\gamma_{zx}^1=\frac{a^2}{\sqrt{z^2-a^2}}\left\{\left[\frac{A_1}{z+\sqrt{z^2-a^2}}+\frac{A_3+\mathrm{i}A_4}{a^2-(z+\sqrt{z^2-a^2})(z_d+\sqrt{z_d^2-a^2})}\right.\right.$$
$$+\frac{A_3-\mathrm{i}A_4}{a^2-(z+\sqrt{z^2-a^2})(\bar{z}_d+\sqrt{\bar{z}_d^2-a^2})}+C_r\frac{e_{15}}{c_{44}}\left[\frac{B_1}{z+\sqrt{z^2-a^2}}\right.$$
$$\left.\left.\left.+\frac{B_3+\mathrm{i}B_4}{a^2-(z+\sqrt{z^2-a^2})(z_d+\sqrt{z_d^2-a^2})}+\frac{B_3-\mathrm{i}B_4}{a^2-(z+\sqrt{z^2-a^2})(\bar{z}_d+\sqrt{\bar{z}_d^2-a^2})}\right]\right]\right\}, \tag{4.9}$$

$$E_y^1+\mathrm{i}E_x^1=-(1-C_r)\frac{a^2}{\sqrt{z^2-a^2}}\left[\frac{B_1}{z+\sqrt{z^2-a^2}}+\frac{B_3+\mathrm{i}B_4}{a^2-(z+\sqrt{z^2-a^2})(z_d+\sqrt{z_d^2-a^2})}\right.$$
$$\left.+\frac{B_3-\mathrm{i}B_4}{a^2-(z+\sqrt{z^2-a^2})(\bar{z}_d+\sqrt{\bar{z}_d^2-a^2})}\right]. \tag{4.10}$$

The related stress and electric displacement fields are then calculated by

$$\tau_{zy}^1+\mathrm{i}\tau_{zx}^1=c_{44}(\gamma_{zy}^1+\mathrm{i}\gamma_{zx}^1)-e_{15}(E_y^1+\mathrm{i}E_x^1), \tag{4.11}$$

$$D_y^1+\mathrm{i}D_x^1=\mathrm{e}_{15}(\gamma_{zy}^1+\mathrm{i}\gamma_{zx}^1)+\varepsilon_{11}(E_y^1+\mathrm{i}E_x^1). \tag{4.12}$$

We found from the above Eqs. (4.9) and (4.10) that the remote loadings along the x-axis γ_{zx}^∞, τ_{zx}^∞, E_x^∞, D_x^∞ contribute nothing to the perturbed fields.

5. Field intensity factors and the energy release rates

The field intensity factors at the right crack tip are defined as

$$K_{\gamma_{zy}}+\mathrm{i}K_{\gamma_{zx}}=\lim_{z\to a}\left[\sqrt{2\pi(z-a)}(\gamma_{zy}+\mathrm{i}\gamma_{zx})\right], \tag{5.1}$$

$$K_{E_y}+\mathrm{i}K_{E_x}=\lim_{z\to a}\left[\sqrt{2\pi(z-a)}(E_y+\mathrm{i}E_x)\right], \tag{5.2}$$

$$K_{\tau_{zy}}+\mathrm{i}K_{\tau_{zx}}=\lim_{z\to a}\left[\sqrt{2\pi(z-a)}(\tau_{zy}+\mathrm{i}\tau_{zx})\right], \tag{5.3}$$

$$K_{D_y}+\mathrm{i}K_{D_x}=\lim_{z\to a}\left[\sqrt{2\pi(z-a)}(D_y+\mathrm{i}D_x)\right]. \tag{5.4}$$

Actually, only $\gamma_{zy}, E_y, \tau_{zy}$ and D_y are singular at the crack tip. The substitution of (4.1)–(4.4) to (5.1)–(5.4) yields

$$K_\gamma = K_{\gamma_{zy}} = \sqrt{\pi a}[A_1 + C_r(e_{15}/c_{44})B_1 - 2C_1(A_3/a + C_r(e_{15}/c_{44})B_3/a) - 2C_2(A_4/a + C_r(e_{15}/c_{44})B_4/a)], \tag{5.5}$$

$$K_E = K_{E_y} = \sqrt{\pi a}(1 - C_r)(-B_1 + 2C_1B_3/a + 2C_2B_4/a), \tag{5.6}$$

$$K_\tau = K_{\tau_{zy}} = \sqrt{\pi a}[c_{44}A_1 + e_{15}B_1 - 2C_1(c_{44}A_3/a + e_{15}B_3/a) - 2C_2(c_{44}A_4/a + e_{15}B_4/a)], \tag{5.7}$$

$$\begin{aligned} K_D = K_{D_y} &= \sqrt{\pi a}[e_{15}A_1 - \varepsilon_{11}B_1 + C_r(e_{15}^2/c_{44} + \varepsilon_{11})B_1 - 2C_1(e_{15}A_3/a - \varepsilon_{11}B_3/a + C_r(e_{15}^2/c_{44} + \varepsilon_{11})B_3/a) \\ &\quad - 2C_2(e_{15}A_4/a - \varepsilon_{11}B_4/a + C_r(e_{15}^2/c_{44} + \varepsilon_{11})B_4/a)], \end{aligned} \tag{5.8}$$

where

$$C_1 = \frac{r_1^* \cos\theta_1 + \sqrt{r_1^* r_2^*}\cos(\theta_1 + \theta_2)/2}{r_1^{*2} + r_1^* r_2^* + 2r_1^*\sqrt{r_1^* r_2^*}\cos(\theta_1 - \theta_2)/2}, \tag{5.9}$$

$$C_2 = \frac{r_1^* \sin\theta_1 + \sqrt{r_1^* r_2^*}\sin(\theta_1 + \theta_2)/2}{r_1^{*2} + r_1^* r_2^* + 2r_1^*\sqrt{r_1^* r_2^*}\cos(\theta_1 - \theta_2)/2} \tag{5.10}$$

with

$$r_1^* = r_1/a, \qquad r_2^* = r_2/a. \tag{5.11}$$

Eq. (5.7) indicates that the stress intensity factor K_τ is not affected by the electric crack condition parameter C_r.

The energy release rate G for the crack propagation can be calculated from the path-independent J integral (Pak, 1990a)

$$G = J = \frac{K_\gamma K_\tau - K_E K_D}{2}. \tag{5.12}$$

6. Image forces on the dislocation

One of the major interests is calculating the image force acting on the dislocation due to the existing of the crack and the remote uniform loadings. The forces acting on the dislocation is a configuration force, which relates the change in energy when the dislocation moves an infinitesimal distance. Following Pak (1990b), the generalized Peach Koehler forces acting on a piezoelectric screw dislocation with a line-force and a line-charge can be written as

$$F_x = b_z\tau_{zy}^{\mathrm{T}} + b_\phi D_y^{\mathrm{T}} + p\gamma_{zx}^{\mathrm{T}} + qE_x^{\mathrm{T}}, \tag{6.1}$$

$$F_y = -b_z\tau_{zx}^{\mathrm{T}} - b_\phi D_x^{\mathrm{T}} + p\gamma_{zy}^{\mathrm{T}} + qE_y^{\mathrm{T}}, \tag{6.2}$$

where the variables σ_{zy}^{T}, σ_{zx}^{T}, D_y^{T}, D_x^{T}, γ_{zy}^{T}, γ_{zx}^{T}, E_y^{T} and E_x^{T} are calculated from Eqs. (4.9), (4.10), (4.11) and (4.12) by taking $z = z_d$. The detail expressions are given by

$$\begin{aligned} \gamma_{zy}^{\mathrm{T}} &= d_1[A_1 + C_r(e_{15}/c_{44})B_1] + (d_3 + d_5)[A_3/a + C_r(e_{15}/c_{44})B_3/a] \\ &\quad + (d_4 - d_6)[A_4/a + C_r(e_{15}/c_{44})B_4/a], \end{aligned} \tag{6.3}$$

$$\gamma_{zx}^{\mathrm{T}} = -d_2[A_1 + C_r(e_{15}/c_{44})B_1] - (d_4 + d_6)[A_3/a + C_r(e_{15}/c_{44})B_3/a] + (d_3 - d_5)[A_4/a + C_r(e_{15}/c_{44})B_4/a], \tag{6.4}$$

$$E_y^{\mathrm{T}} = (1 - C_r)[-d_1B_1 - (d_3 + d_5)B_3/a - (d_4 - d_6)B_4/a], \tag{6.5}$$

$$E_x^{\mathrm{T}} = (1 - C_r)[d_2B_1 + (d_4 + d_6)B_3/a - (d_3 - d_5)B_4/a], \tag{6.6}$$

$$\tau_{zy}^{\mathrm{T}} = d_1(c_{44}A_1 + e_{15}B_1) + (d_3 + d_5)(c_{44}A_3/a + e_{15}B_3/a) + (d_4 - d_6)(c_{44}A_4/a + e_{15}B_4/a), \tag{6.7}$$

$$\tau_{zx}^{\mathrm{T}} = -d_2(c_{44}A_1 + e_{15}B_1) - (d_4 + d_6)(c_{44}A_3/a + e_{15}B_3/a) + (d_3 - d_5)(c_{44}A_4/a + e_{15}B_4/a), \tag{6.8}$$

$$D_y^{\mathrm{T}} = d_1(e_{15}A_1 - \varepsilon_{11}B_1 + C_r(e_{15}^2/c_{44} + \varepsilon_{11})B_1) + (d_3 + d_5)(e_{15}A_3/a - \varepsilon_{11}B_3/a + C_r(e_{15}^2/c_{44} + \varepsilon_{11})B_3/a) + (d_4 - d_6)(e_{15}A_4/a - \varepsilon_{11}B_4/a + C_r(e_{15}^2/c_{44} + \varepsilon_{11})B_4/a), \tag{6.9}$$

$$D_x^{\mathrm{T}} = -d_2(e_{15}A_1 - \varepsilon_{11}B_1 + C_r(e_{15}^2/c_{44} + \varepsilon_{11})B_1) - (d_4 + d_6)(e_{15}A_3/a - \varepsilon_{11}B_3/a + C_r(e_{15}^2/c_{44} + \varepsilon_{11})B_3/a) + C_r(e_{15}^2/c_{44} + \varepsilon_{11})B_3/a + (d_3 - d_5)(e_{15}A_4/a - \varepsilon_{11}B_4/a + C_r(e_{15}^2/c_{44} + \varepsilon_{11})B_4/a + C_r(e_{15}^2/c_{44} + \varepsilon_{11})B_4/a). \tag{6.10}$$

The variables d_1, d_2, d_3, d_4, d_5 and d_6 in the above expressions are

$$d_1 = \frac{r_d^* \cos\left(\theta_d + \frac{\theta_1+\theta_2}{2}\right) + \sqrt{r_1^* r_2^*}\cos(\theta_1 + \theta_2)}{\sqrt{r_1^* r_2^*}\left[r_d^{*2} + r_1^* r_2^* + 2r_d^*\sqrt{r_1^* r_2^*}\cos\left(\theta_d - \frac{\theta_1+\theta_2}{2}\right)\right]}, \tag{6.11}$$

$$d_2 = \frac{r_d^* \sin\left(\theta_d + \frac{\theta_1+\theta_2}{2}\right) + \sqrt{r_1^* r_2^*}\sin(\theta_1 + \theta_2)}{\sqrt{r_1^* r_2^*}\left[r_d^{*2} + r_1^* r_2^* + 2r_d^*\sqrt{r_1^* r_2^*}\cos\left(\theta_d - \frac{\theta_1+\theta_2}{2}\right)\right]}, \tag{6.12}$$

$$d_3 = -\frac{r_d^* \cos(\theta_d + \theta_1 + \theta_2) + \sqrt{r_1^* r_2^*}\cos\frac{3(\theta_1+\theta_2)}{2}}{2r_1^* r_2^*\left[r_d^{*2} + r_1^* r_2^* + 2r_d^*\sqrt{r_1^* r_2^*}\cos\left(\theta_d - \frac{\theta_1+\theta_2}{2}\right)\right]}, \tag{6.13}$$

$$d_4 = -\frac{r_d^* \sin(\theta_d + \theta_1 + \theta_2) + \sqrt{r_1^* r_2^*}\sin\frac{3(\theta_1+\theta_2)}{2}}{2r_1^* r_2^*\left[r_d^{*2} + r_1^* r_2^* + 2r_d^*\sqrt{r_1^* r_2^*}\cos\left(\theta_d - \frac{\theta_1+\theta_2}{2}\right)\right]}, \tag{6.14}$$

$$d_5 = \frac{\cos\left(\frac{\theta_1+\theta_2}{2}\right)}{\sqrt{r_1^* r_2^*}\left[1 - r_d^{*2} - r_1^* r_2^* - 2r_d^*\sqrt{r_1^* r_2^*}\cos\left(\theta_d - \frac{\theta_1+\theta_2}{2}\right)\right]}, \tag{6.15}$$

$$d_6 = \frac{\sin\left(\frac{\theta_1+\theta_2}{2}\right)}{\sqrt{r_1^* r_2^*}\left[1 - r_d^{*2} - r_1^* r_2^* - 2r_d^*\sqrt{r_1^* r_2^*}\cos\left(\theta_d - \frac{\theta_1+\theta_2}{2}\right)\right]} \tag{6.16}$$

with

$$r_d^* = r_d/a, \tag{6.17}$$

where r_d in Eq. (6.17) and r_1, r_2 in Eq. (5.11) are shown in Fig. 1.

7. Numerical examples and discussions

In this section, numerical examples are performed to show how the electric crack condition parameter C_r affects the energy release rate and the forces on the dislocation. There are four different remote applied loadings (γ_{zy}^{∞}, τ_{zy}^{∞}, E_y^{∞}, D_y^{∞}). To simplify the numerical calculations, only the case when the remote applied loadings are τ_{zy}^{∞}, E_y^{∞} (i.e., Case a, in Section 3) is discussed here. As for the dislocation, there are four different dislocation strength characteristics (b_z, b_φ, p, q) and two dislocation position characteristics (r_d, θ_d). To plot the results in normalized forms, we allow the dislocation to have only one none-zero strength characteristic and the other three are zero in each plotted curve. A PZT-6B material is used in the calculations, whose material properties are

$$c_{44} = 2.71 \times 10^{10}\ \mathrm{N/m^2}, \qquad e_{15} = 4.6\ \mathrm{C/m^2}, \qquad \varepsilon_{11} = 3.6 \times 10^{-9}\ \mathrm{C/V\,m}. \tag{7.1}$$

7.1. The energy release rates

The energy release rate for the crack under remote uniform loadings τ_{zy}^{∞}, E_y^{∞} can be obtained as

$$G = \frac{1}{2}\frac{\pi a(\tau_{zy}^{\infty})^2}{c_{44}}\left[1 - (1 - C_r)(c_{44}\varepsilon_{11} + e_{15}^2)\left(\frac{E_y^{\infty}}{\tau_{zy}^{\infty}}\right)^2\right]. \tag{7.2}$$

Eqs. (7.2) and (7.3) indicate that, the electric loading always impedes crack propagation for the electrically impermeable crack $C_r = 0$ (Pak, 1990a), while, does not affect crack propagation for the electrically permeable crack $C_r = 1$ (McMeeking, 1989; Zhang and Tong, 1996).

The influences of the dislocation on the energy release rates are not straightforward. The electrically crack condition parameter C_r does not affect $G^*(b_z)$, but it has significant influence on $G^*(b_\varphi)$, $G^*(p)$ and $G^*(q)$, as shown in Fig. 2, where, as an example, the dislocation is fixed at $(r_d, \theta_d) = (1.1a, \pi/10)$. Fig. 3 illustrates how C_r influences on $G^*(b_\varphi)$ when r_d is fixed at $1.1a$, where $G^*(b_\varphi)$ is depicted varied with the polar anger of the dislocation θ_d. The normalizing factors in each curve of the above figures are given separately by

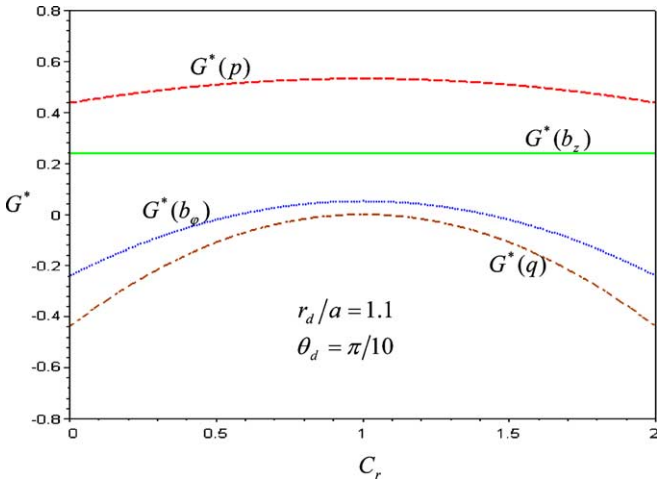

Fig. 2. The variation in the normalized energy release rate G/G_0 with C_r when dislocation is located at $(r_d, \theta_d) = (1.1a, \pi/10)$.

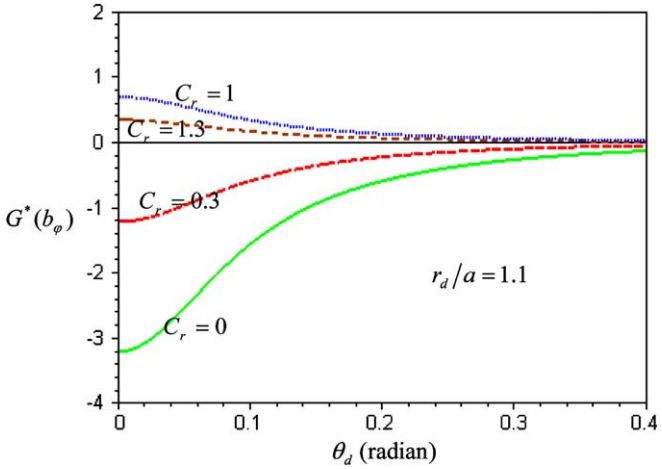

Fig. 3. The variation in the normalized energy release rate $G(b_\varphi)/G_0(b_\varphi)$ with the polar anger θ_d when $r_d = 1.1a$.

$$G_0(b_z) = \frac{c_{44}b_z^2}{2\pi a}, \qquad G_0(b_\varphi) = \frac{\varepsilon_{11}b_\varphi^2}{2\pi a}, \qquad G_0(p) = \frac{p^2}{2\pi a c_{44}}, \qquad G_0(q) = \frac{q^2}{2\pi a \varepsilon_{11}}. \tag{7.3}$$

For example, $G^*(b_\varphi)$ in the figures can be expressed as $G(b_\varphi)/G_0(b_\varphi)$, where $G(b_\varphi)$ is the energy release rate due to a dislocation with only non-zero strength characteristic b_φ.

Fig. 3 shows that for $C_r = 0$ (electrically impermeable assumption) and $C_r = 0.3$, the electric potential dislocation b_φ accelerates the crack propagation. However, for $C_r = 0$ (an electrically permeable assumption) and $C_r = 1.3$, the electric potential dislocation b_φ retards the crack propagation.

7.2. The image forces

As described in Section 6, the image forces on the dislocation due to the existing of the crack and the remote uniform loadings are calculated in Eqs. (6.1) and (6.2). As a numerical example, we just plot the image slip force,

$$F_r = F_x \cos\theta_d + F_y \sin\theta_d, \tag{7.4}$$

here and the following values for the dislocation characteristics are used:

$$b_z = 1.0 \times 10^{-9}\ \text{m}, \qquad b_\varphi = 1.0\ \text{V}, \qquad p = 10\ \text{N/m}, \qquad q = 1.0 \times 10^{-8}\ \text{C/m}. \tag{7.5}$$

The remote uniform shear stress and the crack sized are assumed to be

$$\tau_{zy}^{\infty} = 1.0 \times 10^{6}\ \text{N/m}^2, \qquad a = 1.0 \times 10^{-6}\ \text{m}. \tag{7.6}$$

In each plotted curve shown in the following, the dislocation has only one none-zero strength characteristic. The normalizing factors in each curve are given separately by

$$F_0(b_z) = \frac{c_{44}b_z^2}{4\pi a}, \qquad F_0(b_\varphi) = \frac{\varepsilon_{11}b_\varphi^2}{4\pi a}, \qquad F_0(p) = \frac{p^2}{4\pi a c_{44}}, \qquad F_0(q) = \frac{q^2}{4\pi a \varepsilon_{11}}. \tag{7.7}$$

Fig. 4 plots the variations in the normalized image slip force F_r/F_0 with the electric crack condition parameter C_r when the dislocation is fixed at $(r_d, \theta_d) = (1.1a, \pi/6)$ and $E_y^{\infty} = -2.0 \times 10^5$ V/m.

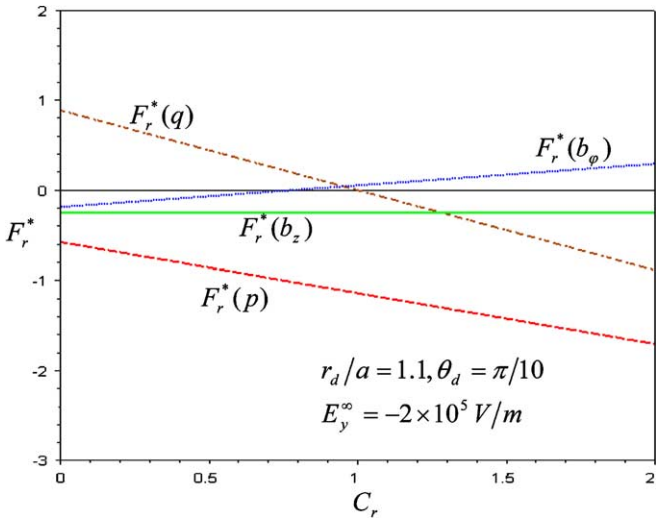

Fig. 4. The variation in the normalized image slip force F_r/F_0 with C_r when dislocation is located at $(r_d, \theta_d) = (1.1a, \pi/6)$ under remote uniform shear stress and electric field.

Fig. 4 shows that under such remote loadings, increasing C_r results in increasing $F_r(b_\varphi)$, but decreasing $F_r(p)$ and $F_r(q)$. Fig. 4 also shows that the electric crack condition parameter does not affect $F_r(b_z)$.

Figs. 5–7 plot the variations of $F_r(b_\varphi)$, $F_r(p)$ and $F_r(q)$, respectively, with the polar anger of the dislocation θ_d under four different electric crack condition parameter C_r. The remote electric field is fixed at $E_y^\infty = -2.0 \times 10^5$ V/m. Fig. 5 shows that in the case that the electric potential dislocation b_φ is initiated near the real axis (θ_d is small), the crack will repel it in the radial direction when $C_r = 0$ or $C_r = 0.3$; while attract

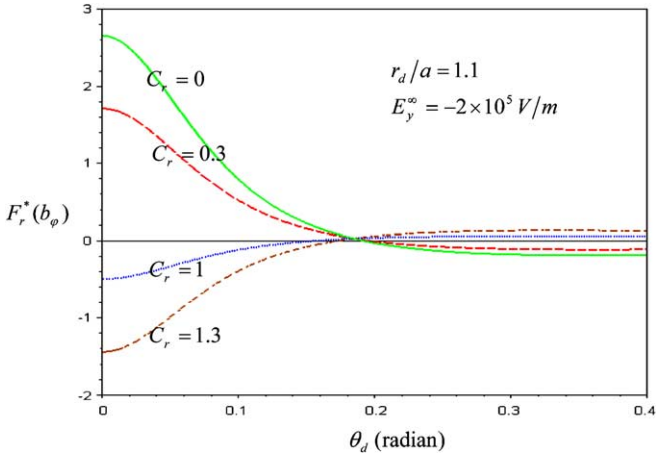

Fig. 5. The variation in the normalized image slip force F_r/F_0 due to b_φ with the polar anger θ_d when $r_d = 1.1a$ under remote uniform shear stress and electric field.

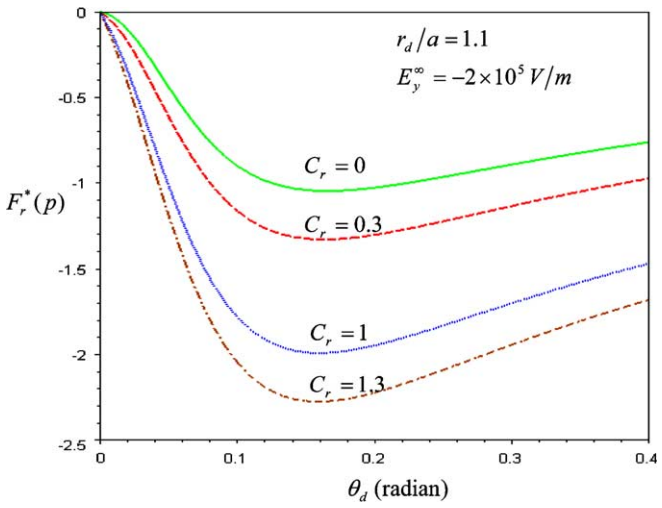

Fig. 6. The variation in the normalized image slip force F_r/F_0 due to line-force p with the polar anger θ_d when $r_d = 1.1a$ under remote uniform shear stress and electric field.

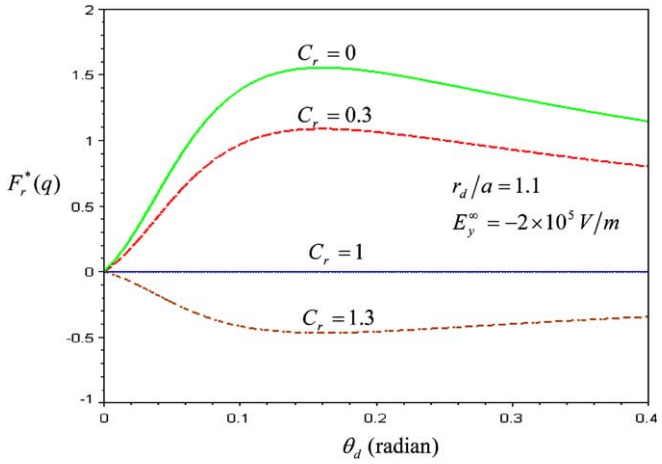

Fig. 7. The variation in the normalized image slip force F_r/F_0 due to line-charge q with the polar anger θ_d when $r_d = 1.1a$ under remote uniform shear stress and electric field.

when $C_r = 1$ or $C_r = 1.3$. As for the line-force p, the crack always attracts it in the radial direction despite of the value of C_r, as shown in Fig. 6. However, the crack repels the line-charge q when $C_r = 0$ or $C_r = 0.3$; attracts it when $C_r = 1.3$; but does not affect it when $C_r = 1$.

In the previous discussion, the remote electric field is fixed at a negative value. In order to examine the influence from the remote electric field, Figs. 8 and 9 plot the variation of the normalized $F_r(b_\varphi)$ with the polar anger of the dislocation θ_d for $C_r = 0.6$ and $C_r = 1.3$, respectively. It is noted that positive remote electric field enhances the magnitudes of the force on the dislocation b_φ.

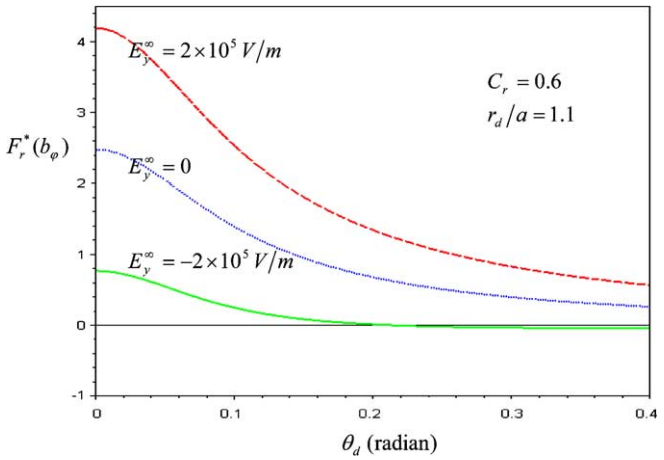

Fig. 8. The variation in the normalized image slip force F_r/F_0 due to b_φ with the polar anger θ_d when $r_d = 1.1a$ and $C_r = 0.6$.

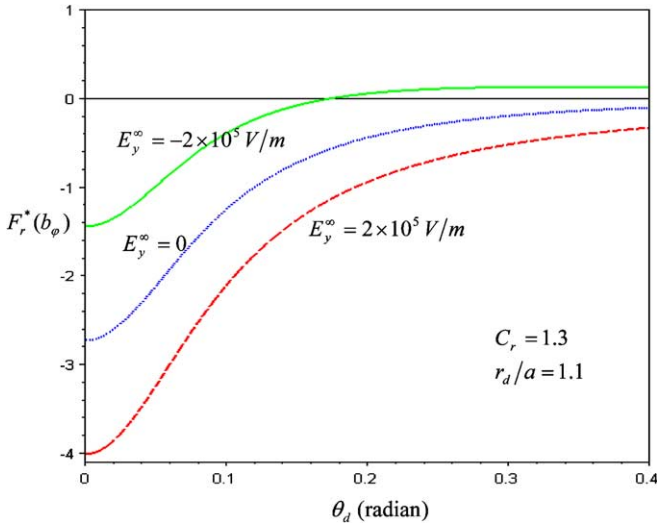

Fig. 9. The variation in the normalized image slip force F_r/F_0 due to b_φ with the polar anger θ_d when $r_d = 1.1a$ and $C_r = 1.3$.

8. Conclusions

The electro-elastic interaction of a piezoelectric screw dislocation, a line-force, and a line-charge near a finite crack in a piezoelectric medium is considered. The analysis is conducted on the electrically unified crack boundary condition with the introduction of the electric crack condition parameter that can describe all the electric crack boundary conditions. The explicit expressions of the mechanical and electrical fields produced by a line-force, a line-charge and a screw dislocation are derived and the field intensity factors are calculated. The image forces on the dislocation due to the crack and the remote uniform loadings are also calculated. The solution can be served as Green's functions for studying crack propagation problems in

piezoelectric media. The two ideal crack boundary conditions, namely, the electrically impermeable and permeable crack assumptions are obtained as two special cases for the current solution. Numerical examples are performed to show how the electric crack condition parameter affects the field intensity factors and the force on the dislocation.

References

Deeg, W.F., 1980. The analysis of dislocation, crack, and inclusion problems in piezoelectric solids. Ph.D. Thesis. Stanford University.

Dunn, M.L., 1994. The effect of crack face boundary conditions on the fracture mechanics of piezoelectric solids. Eng. Fract. Mech. 48, 25–39.

Kwon, J.H., Lee, K.Y., 2002. Electromechanical effect of a screw dislocation around a finite crack in a piezoelectric material. Trans. ASME J. Appl. Mech. 69, 55–62.

Kwon, S.M., 2003. Electrical nonlinear anti-plane shear crack in a functionally graded piezoelectric strip. Int. J. Solids Struct. 40, 5649–5667.

McMeeking, R.M., 1989. Electrostrictive stresses near crack-like flaws. J. Appl. Math. Phys. (ZAMM) 40, 615–627.

Muskhelishvili, N.I., 1975. Some Basic Problems of the Mathematical Theory of Elasticity. Noordhoff International Publishing, Leyden.

Pak, Y.E., 1990a. Crack extension force in a piezoelectric material. Trans. ASME J. Appl. Mech. 57, 647–653.

Pak, Y.E., 1990b. Force on a piezoelectric screw dislocation. Trans. ASME J. Appl. Mech. 57, 863–869.

Pak, Y.E., 1992. Linear electro-elastic fracture mechanics of piezoelectric materials. Int. J. Fract. 54, 79–100.

Park, S.B., Sun, C.T., 1995. Effect of electric field on fracture of piezoelectric ceramics. Int. J. Fract. 70, 203–216.

Parton, V.Z., 1976. Fracture mechanics of piezoelectric materials. Acta Astronaut. 3, 671–683.

Qin, Q.H., Yu, S.W., 1997. An arbitrarily-oriented plane crack terminating at the interface between dissimilar piezoelectric materials. Int. J. Solids Struct. 34, 581–590.

Qin, Q.H., 2000. General solutions for thermopiezoelectrics with various holes under thermal loading. Int. J. Solids Struct. 37, 5561–5578.

Sosa, H.A., 1991. Plane problems in piezoelectric media with defects. Int. J. Solids Struct. 28, 491–505.

Sosa, H.A., Khutoryansky, N., 1996. New developments concerning piezoelectric materials with defects. Int. J. Solids Struct. 33, 3399–3414.

Wang, B., 1992. Three-dimensional analysis of a flat elliptical crack in a piezoelectric medium. Int. J. Eng. Sci. 30, 781–791.

Wang, B.L., Mai, Y.W., 2003. On the electrical boundary conditions on the crack surfaces in piezoelectric ceramics. Int. J. Eng. Sci. 41, 633–652.

Zhang, T.Y., Tong, P., 1996. Fracture mechanics for a mode III crack in a piezoelectric material. Int. J. Solids Struct. 33, 343–359.

Zhang, T.Y., Qian, C.F., Tong, P., 1998. Linear electric-elastic analysis of a cavity or a crack in a piezoelectric material. Int. J. Solids Struct. 35, 2121–2149.

Zhang, T.Y., Wang, T.H., Zhao, M.H., 2002. Interaction of a piezoelectric screw dislocation with an insulting crack. Philos. Mag. 82, 2805–2824.

Zhong, Z., Meguid, S.A., 1997a. Interfacial debonding of a circular inhomogeneity in piezoelectric materials. Int. J. Solids Struct. 34, 1965–1984.

Zhong, Z., Meguid, S.A., 1997b. Analysis of a circular arc-crack in piezoelectric materials. Int. J. Fract. 84, 143–158.